Wide Post-Mass Transfer White-Dwarf Binaries

Runqiu Ye

June, 2024

1 Introduction

Common envelope (CE) is the outcome of unstable mass transfer. During CE, both stars orbit inside an envelope and spiral inward. If the energy liberated in this process is enough to eject the CE, then the result of CE process is a close binary. If, on the contrary, the liberated energy is not enough to eject the envelope, then the result of the process is a merger. In observation results, a number of WD+MS binaries are wider than expected, and CE is expected to be the main channel to form these white dwarf binaries [YEBF$^+$24, YEBR$^+$24]. In the MESA model utilized by [YEBF$^+$24, YEBR$^+$24], wide post-CE WD+MS binaries can be formed in a certain range of initial separation with only gravitational and internal energy included in the calculation.

In this paper, we are going to explore the formation possibility of these wide post-mass transfer WD+MS binaries with COSMIC model. We perform COSMIC simulation on both individual binary star systems and sampled population to explore the formation of WD+MS binaries under different conditions. In section 2, we are going to investigate formation of individual wide WD+MS binaries through CE for a variety of variables, including initial mass, initial separation, CE efficiency, and the energy budget of the CE. In section 3, we are going to explore the formation of individual wide WD+MS binaries through stable mass transfer. In section 4, we will research on how different COSMIC model affect simulation results of a sample population of binary star systems, and how the formation of post WD+MS binaries depends on various parameters.

2 Formation Through Common Envelope

In [YEBF$^+$24, YEBR$^+$24], the author discussed the formation of WD+MS binaries through CE for both high-mass and low-mass systems, and it was found that wide WD+MS systems can be formed for certain energy budgets and certain initial separation in the MESA model. We hope to explore similar models in COSMIC.

In [YEBF$^+$24, YEBR$^+$24], to explore the dependency of the final separation a_f in the post-CE binary on the initial separation a_i in the pre-MT binary, the author first run a stellar evolution model of the primary star using MESA. Its evolution up to AGB phase is followed. With the model, the binding energy of the CE is calculated as

$$E_{\rm bind} = E_{\rm grav} + E_{\rm int} = \int_{M_{\rm core}}^{M_{\rm tot}} -\frac{Gm}{r(m)} + U(m)dm, \tag{1}$$

or

$$E_{\rm bind} = E_{\rm grav} + \alpha_{\rm th}E_{\rm th} + \alpha_{\rm rec}E_{\rm rec}. \tag{2}$$

After that, the change of separation through CE evolution is calculated using

$$E_{\rm bind} = \alpha_{\rm CE}\left(-\frac{GM_{\rm WD}M_\star}{2a_f} + \frac{GM_iM_\star}{2a_i}\right). \tag{3}$$

In COSMIC, the CE is modeled using a structural parameter λ, where

$$E_{\rm bind} = \frac{GM_iM_{\rm env}}{\lambda R_i}. \tag{4}$$

This λ is represented in COSMIC as the `lambdaf` flag in `BSEDict`. To compare MESA model with COSMIC, we intend to compare how the energy budget utilized by [YEBF$^+$24, YEBR$^+$24] matches with the CE model in COSMIC. We approach this by calculating the effective λ value for each of the common envelope energy budget used in [YEBF$^+$24, YEBR$^+$24].

2.1 High Mass Systems ($7\,\mathrm{M}_\odot + 1\,\mathrm{M}_\odot$)

2.1.1 Methods and results

According to [YEBF$^+$24], the lower limit of WD mass $M_{\rm MD,min}$ in the observational sample is calculated to be $1.244\,\mathrm{M}_\odot \sim 1.418\,\mathrm{M}_\odot$. The corresponding mass of MS progenitor is expected to be in the range of $6 \sim 9\,\mathrm{M}_\odot$, and the companion mass has median around $1\,\mathrm{M}_\odot$. MESA results for $7\,\mathrm{M}_\odot + 1\,\mathrm{M}_\odot$ systems is documented in [YEBF$^+$24]. Hence, we also consider a $7\,\mathrm{M}_\odot + 1\,\mathrm{M}_\odot$ evolution model in COSMIC and compare the results with those in [YEBF$^+$24].

We run COSMIC binary evolution simulation of a $7\,\mathrm{M}_\odot + 1\,\mathrm{M}_\odot$ system and investigate how the final separation a_f depends on the initial separation a_i and the CE parameter λ. The initial separation is a linear grid in range $2 \sim 8\,$au with 400 points. The CE flag `lambdaf` is a linear grid in range $0 \sim -100$ with 2000 steps, which corresponds to $0 \sim 100$ for CE parameter λ. Also, we run these parameters with four different CE efficiencies — $\alpha_{\rm CE} = 1$, $\alpha_{\rm CE} = 0.9$, $\alpha_{\rm CE} = 0.6$, and $\alpha_{\rm CE} = 0.3$, the same as recorded in [YEBF$^+$24]. In total, for each of the 4 different CE efficiency $\alpha_{\rm CE}$, we run a grid of 80000 binary star systems with different initial separation a_i and CE parameter λ.

After simulation is finished, we select the time-step when the system finished CE for the first time (`evol_type=8`). At this moment, if the system is a WD+MS system, we record their separation as the final separation a_f. Otherwise, we set $a_f = 0$ and consider this initial condition unable to produce a WD+MS system. We create four heat maps for the four different CE efficiencies. In Figure 1, we plot the final separation a_f of the WD+MS systems against initial separation a_i and the CE flag $-\lambda$.

2.1.2 Discussions

There are several interesting points of the results. First of all, comparing the four panels, we found that as $\alpha_{\rm CE}$ decreases, the final separation decreases in general. This can be explained by Equation 3. Qualitatively, note that more energy from the orbit is needed to eject the envelope for low $\alpha_{\rm CE}$, so the resulting a_f is expected to be smaller.

It is worth noting that most of these systems experience two mass transfer phases in COSMIC before reaching WD+MS. That is, during the evolution process, two CE processes take place, between which there is a period of time. A typical change of `evol_type` through the evolution is **...-3-7-8-4-...-3-7-8-4-...**, where WD+MS is reached during the second mass transfer process. Another possible change of `evol_type` through the volution is **...-3-7-8-7-8-4-...**, which will be mentioned in the next paragraph. Statistically, we found that **(***TO-DO***)** fraction of all our 320000 simulated binaries experience two CE processes before reaching WD+MS. To explain this qualitatively, we notice that

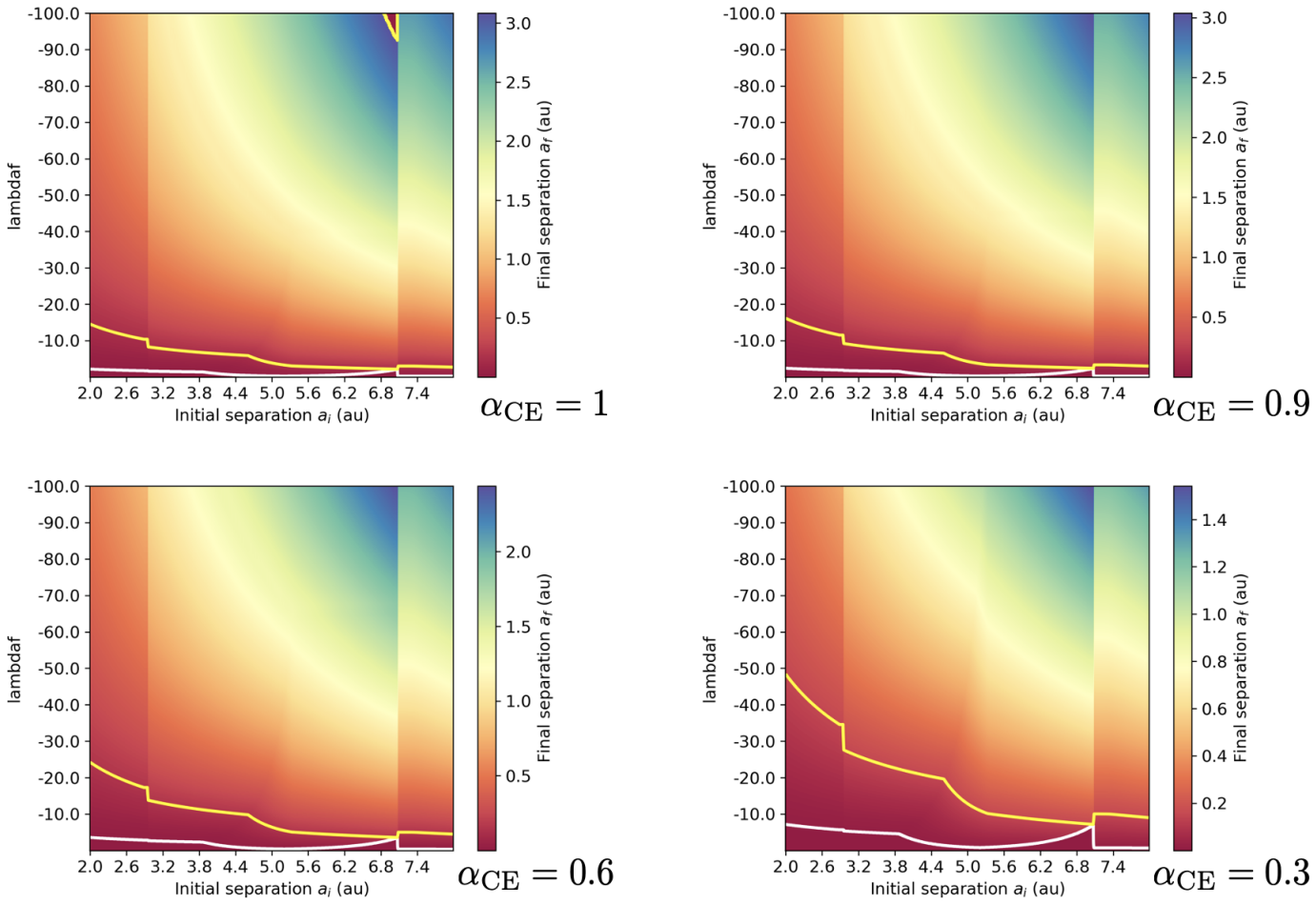

Figure 1: Heat map of final separation a_f against initial separation a_i and CE flag $-\lambda$. Different panels represent four different CE efficiencies $\alpha_{\rm CE} = 1$, 0.9, 0.6, and 0.3. The white and yellow contour corresponds to $a_f = 0.01\,$au and $a_f = 0.15\,$au respectively. WD+MS binaries is not possible for separation smaller than 0.01 au, and 0.15 au is the minimum separation of wide WD+MS binaries in observational results. Outside the white contour no desired system forms.

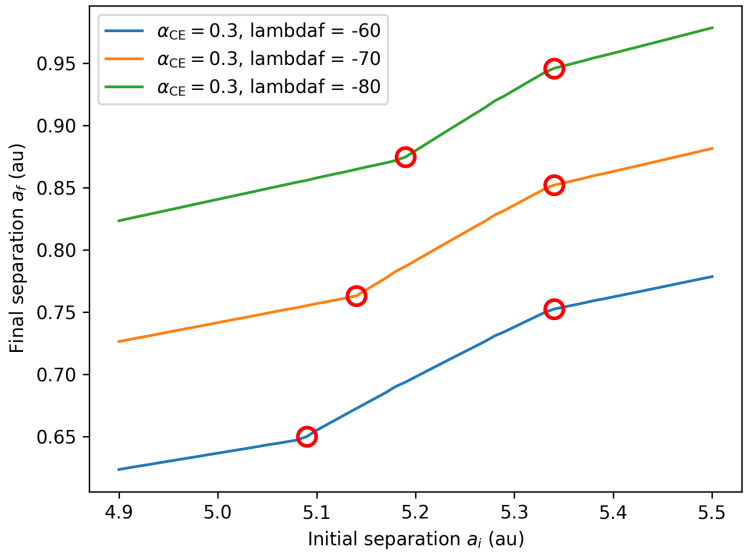

Figure 2: Dependence of final separation a_f on initial separation a_i for $\alpha_{\rm CE} = 0.3$. Simulation results of $\lambda_f = 60$, 70, and 80 are shown. The red circles emphasizes the jump of final separation as initial separation increases.

when the primary loses too much mass during the first CE, the CE process ends, as the radius of the primary becomes smaller than the Roche Lobe. After the primary fills its Roche lobe and has a large enough envelope again, the CE process resumes and causes two CE processes in total.

From Figure 1, we also notice that final separation a_f jumps obviously at about 2.9 au, and 7.1 au. After investigating the `bpp` array of these simulations, we find out the jump at about 2.9 au and 7.1 au is likely due to the difference of `kstar_1` at the start of RLOF. For $a_i < 2.9$ au, RLOF starts when `kstar_1=3`. For $a_i = 2.9$ au, RLOF starts when `kstar_1=4`. For $2.9\,{\rm au} < a_i < 7.1\,{\rm au}$, RLOF starts when `kstar_1=5`. For $a_i > 7.1$ au, RLOF starts when `kstar_1=6`. For different star type, the structure and mass of the envelope is different, leading to different binding energy $E_{\rm bind}$ and thus different final separation a_f.

Inspecting more closely, we found that the final separation a_f jumps at about $5.2 \sim 5.4$ au. This is especially obvious with $\alpha_{\rm CE} = 0.3$. To illustrate, we zoom in the simulation results of $\alpha_{\rm CE} = 0.3$, and present the change of final separation a_f as initial separation a_i increases in Figure 2. From here, we can clearly see two jumps — one between 5.1 au and 5.2 au, the other at 5.34 au. To explain this, we again go to the `bpp` array of these systems. The first jump is because the evolution process changes from **3-7-8-4-3-7-8-4** to **3-7-8-7-8-4**. This means that for relatively larger initial separation a_i, the primary fills its Roche lobe all the time, leading to more mass loss during a shorter timescale and thus larger final separation. For the second jump, it is because `kstar_1` changes from `8` to `9` at the start of the second common envelope. This changes the binding energy of the common envelope and thus changes the final separation.

Finally, notice that there exists a small triangular gap in the figure for $\alpha_{\rm CE} = 1$. This is because `kstar_1` becomes a neutron star and no rows in the `bpp` gets selected.

In conclusion, with a large `lambdaf`, it is possible to create wide post-mass transfer WD+MS systems with final separation $a_f > 0.15$ au, which is the minimal separation of our observed objects. In next section, we will compare these results with default settings in COSMIC and with results in [YEBF$^+$24], in order to investigate the possibility of forming wide WD+MS systems through CE.

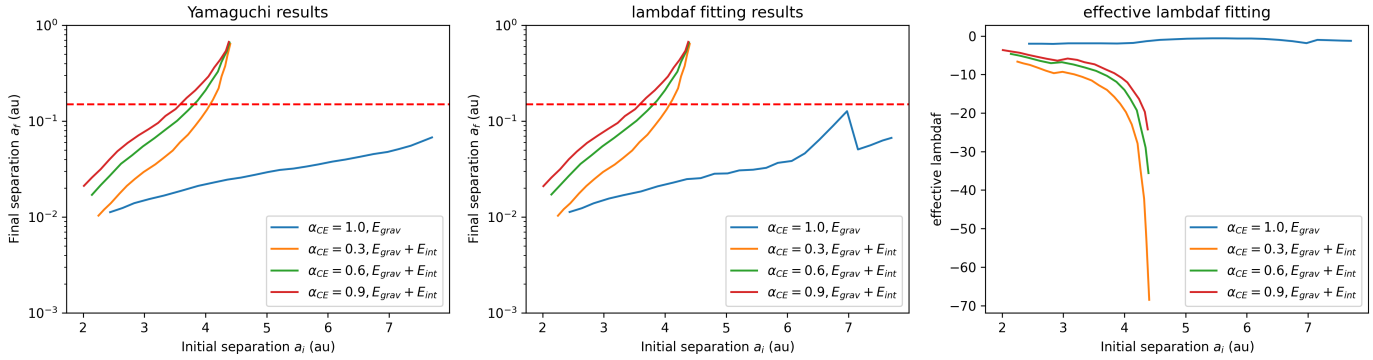

Figure 3: Effective λ fitting results of a $7\,M_\odot + 1\,M_\odot$ system for common envelope structure in MESA. Different lines represent different $\alpha_{\rm CE}$ and different common envelope energy budget, as shown in the legend. Left panel: MESA results in [YEBF+24] of how final separation a_f depends on initial separation a_i. Central panel: COSMIC results of how final separation a_f depends on initial separation a_i, produced by the effective λ calculated. Right panel: effective λ in COSMIC that corresponds to the MESA results for each initial separation a_i. The red dashed line in the left and middle panel represents 0.15 au, which is the minimal separation for observed wide post-CE WD+MS binaries.

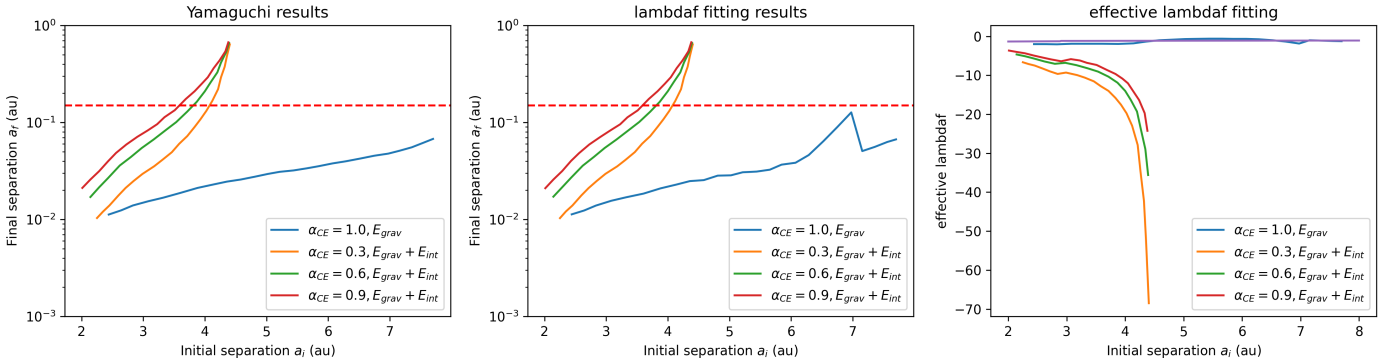

Figure 4: Same as Figure 3, but with default λ in COSMIC model included in the right panel.

2.1.3 Comparison

After we have obtained the simulation results for different initial conditions, now we can calculate the effective λ that matches with results in [YEBF+24]. For each fixed initial separation a_i, we loop through the COSMIC results with the same initial separation, and find the `lambdaf` value that results in a final separation closest to MESA model results. We record this `lambdaf` as the effective λ that matches the binding energy formalism at initial separation a_i.

We present the fitting results for energy budget $E_{\rm bind} = E_{\rm grav} + E_{\rm int}$ in Figure 3. Notice that in the central panel, there is a small bump of the blue line. This is because at $6 \sim 7$ au, we cannot reach such low final separation in COSMIC while forming a WD+MS binary at the same time. From the left panel, we can see that it is possible to create WD+MS binaries with final separation > 0.15 au in MESA as long as internal energy $E_{\rm int}$ is included. However, in the right panel we show that this correspond to very large `lambdaf` in COSMIC ($\lambda >\sim 20$).

To further compare with the default λ value in COSMIC, we include in the right panel an extra line which represents the default λ value in COSMIC. This default λ in the COSMIC model is calculated following Appendix A of [CPI+14]. For all of our case, we have $M_{\rm env} > 1$. The results is shown in Figure 4. Notice that the default λ value is at order ~ 1, far smaller than the effective λ needed to recreate results in [YEBF+24]. Hence, we conclude that in COSMIC, it is not practical to form wide high mass

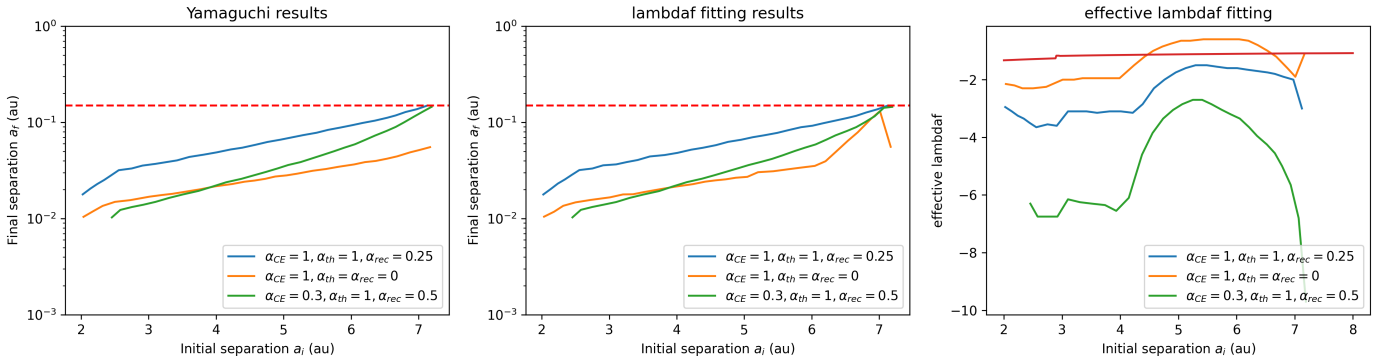

Figure 5: Same as Figure 4, but with a different common envelope energy budget. For results shown in these figures, $E_{\rm bind} = E_{\rm grav} + \alpha_{\rm th} E_{\rm th} + \alpha_{\rm rec} E_{\rm rec}$, where the coefficients $\alpha_{\rm th}$ and $\alpha_{\rm rec}$ for different line is shown in the legend.

WD+MS system through common envelope processes, since the required λ is too large.

In Figure 5, we present the same results for another energy budget of the CE process. Rather than including both thermal and recombination energy into the binding energy, we use two coefficients $\alpha_{\rm th}$ and $\alpha_{\rm rec}$ to consider their contribution to $E_{\rm bind}$ separately. That is,

$$E_{\rm bind} = E_{\rm grav} + \alpha_{\rm th} E_{\rm th} + \alpha_{\rm rec} E_{\rm rec}.$$

We notice that the effective λ now gets with in the order of $\sim$ 10. However, none of these initial separation and λ results in wide WD+MS system with final separation $a_f > 0.15\,$au. Therefore, we conclude that with the new energy budget, it is not practical to form wide WD+MS binaries either.

2.2 Low Mass Systems $(1.5\,{\rm M}_\odot + 0.85\,{\rm M}_\odot)$

In [YEBR+24], the WD mass in the Gaia sample ranges from $0.5\,{\rm M}_\odot$ to $0.8\,{\rm M}_\odot$, which corresponds to progenitor mass of $1\,{\rm M}_\odot$ to $3\,{\rm M}_\odot$. The companions mass has a median of $0.85\,{\rm M}_\odot$. MESA results for $1.5\,{\rm M}_\odot + 0.85\,{\rm M}_\odot$ systems is documented in [YEBF+24]. Hence, we consider a $1.5\,{\rm M}_\odot + 0.85\,{\rm M}_\odot$ evolution model in COSMIC and compare the results with those in [YEBF+24].

3 Formation Through Stable Mass Transfer

4 Population Synthesis Results

References

[CPI+14] JSW Claeys, OR Pols, RG Izzard, J Vink, and FWM Verbunt. Theoretical uncertainties of the type ia supernova rate. *Astronomy & Astrophysics*, 563:A83, 2014.

[YEBF+24] Natsuko Yamaguchi, Kareem El-Badry, Jim Fuller, David W Latham, Phillip A Cargile, Tsevi Mazeh, Sahar Shahaf, Allyson Bieryla, Lars A Buchhave, and Melissa Hobson. Wide post-common envelope binaries containing ultramassive white dwarfs: evidence for efficient envelope ejection in massive asymptotic giant branch stars. *Monthly Notices of the Royal Astronomical Society*, 527(4):11719–11739, 2024.

[YEBR+24] Natsuko Yamaguchi, Kareem El-Badry, Natalie Rees, Sahar Shahaf, Tsevi Mazeh, and René Andrae. Wide post-common envelope binaries from gaia: orbit validation and formation models. *arXiv preprint arXiv:2405.06020*, 2024.